Piotr SOBAŃSKI

Wroclaw University of Technology, Department of Electrical Machines, Drives and Measurements

doi:10.15199/48.2016.05.14

IGBTs Open-Circuit Faults Diagnostic Methods for the Voltage Inverter Fed Induction Motor Drives

***Abstract**. In this paper an effectiveness of IGBTs open-circuit faults diagnostic methods, that are based on vector hodographs analysis, for the two-level three-phase voltage inverter fed induction motor drive, are investigated. In accordance with the research, whose chosen results have been presented in this work, two diagnostic techniques have been validated experimentally in the direct rotor field oriented control as well as direct torque control induction motor drive. The conducted study has a comparative dimension and aims to assess the effectiveness, robustness against false alarms and speed of the fault diagnosis of the algorithms based on a rotor or stator flux estimation, depending on the control structure, or method that takes into consideration a reference voltage vector of the inverter. Additionally, simplified implementation schemes of the diagnostic systems have been presented.*

***Streszczenie.** W artykule zweryfikowano skuteczność działania metod diagnostyki uszkodzeń polegających na braku przewodzenia prądu tranzystorów w dwupoziomowym, trójfazowym falowniku napięcia zasilającym napęd z silnikiem indukcyjnym. Prezentowane algorytmy zostały oparte na analizie hodografów wybranych zmiennych stanu napędu w układzie bezpośredniego sterowania polowo zorientowanego ze strumieniem wirnika oraz bezpośredniego sterowania momentem elektromagnetycznym. Celem przeprowadzonych badań, które mają charakter porównawczy, jest weryfikacja skuteczności diagnozy, odporności na generowanie fałszywych alarmów oraz szybkości lokalizacji nieprawidłowo funkcjonujących tranzystorów, w przypadku analizowanych metod diagnostycznych, opartych na estymowanym strumieniu wirnika bądź stojana oraz algorytmu, w którym jest wykorzystywany wektora zadanego napięcia falownika. W artykule zaprezentowano również proste metody realizacji praktycznej systemów diagnostyki awarii tranzystorów. (**Metody diagnostyki uszkodzeń polegających na braku przewodzenia prądu tranzystorów IGBT w napędach z silnikiem indukcyjnym zasilanym z falownika napięcia**).*

Keywords: induction motor, voltage inverter, IGBT fault diagnosis.
Słowa kluczowe: silnik indukcyjny, falownik napięcia, diagnostyka uszkodzeń tranzystorów IGBT.

Introduction

The most of electric motor drive system malfunctions deal with power converter failures, resulting in a significant decrease of a drive performance [1]-[3]. Along with DC-link capacitor faults, that make up more than 60% deviations, that are related to the power converters [4], IGBTs transistor failures are the vast majority ones. These faults are mainly caused by an ageing process, which is intensified due to a thermal stress of the transistors, when the inverter operates under wide range of environment temperature variations and a changeable load condition [5]. From two types of the transistor malfunctions, namely short- and open-circuit faults, the first ones are more destructive for the power converters than the second ones because they can result in a high current flow thru the DC-link circuit and a complementary transistor of the faulty converter phase, which leads to a capacitors destruction. In this case, a power converter protection is realized by specialized transistor gate drivers which turn off the faulty transistors immediately, when the failures happen. As a result, the faulted switch does not conduct the current similarly when the open-circuit failure occurs. The second reason of the loss of transistor current conducting capability are the IGBT gate driver malfunctions as well as physical semiconductor failures [6]. Since these malfunctions result unacceptable errors of controlled motor drive state variables, specialized control techniques, known as fault-tolerant control methods (FTCM), which allow an uninterrupted electric drive operation under its faulty condition, have been developed recently [7]-[11]. According to FTCM, a remedial action, that brings back a full or partial drive functionality, is carried out by using an information about a localization of the faulted switch. Thus, it is important to recognize the affected transistor correctly and fast. The open-circuit fault diagnostic methods have been developed for many years and they can be divided into two groups, namely techniques based on hardware solutions and algorithms, that do not require extra measurement systems installation for the fault diagnosis.

The hardware-based methods consist in an error calculation between expected voltages and the measured ones. However, these techniques, despite having very short time of the failure localization, they require a relatively high sampling time of a control system to avoid a false diagnosis caused by the switching death time [6], [12]-[16]

A clear majority of the open-circuit faults diagnostic methods are based on software ideas, which significantly decrease implementation cost of the fault monitoring system. Many of them rely on calculating of standardized errors between reference, estimated or measured diagnostic variables [17]-[22]. As a result of IGBT open-circuit failure, voltages of the inverter are estimated incorrectly, which is a reason of wrong stator currents or flux calculations, respectively to the diagnostic method. According to these techniques, the average values of the incorrectly estimated diagnostic variables are compared with the measured ones or with the results obtained by using current-based estimators, which are not affected by the transistor malfunctions. To determine the faulted switch the diagnostic variables are compared with a fault threshold that should by assumed experimentally. The second group of the open-circuit fault diagnostic methods are the algorithms based on an analysis of vector transient of chosen drive state variables, which are defined in the stationary reference frame $\alpha-\beta$ [2], [23]-[30]. The vast majority of these techniques use stator currents for the faults diagnosis [23]-[28] so they are sensitive to load variations. Therefore, to overcome this disadvantage standardization techniques can be utilized, namely the stator phase currents are divided by an amplitude of the current space vector. The fault localization procedure takes more time than in case of previously described methods, that are based on the residues, and can be longer than one period of the current fundamental harmonic.

In this article address the comparison of IGBTs open-circuit faults diagnostic techniques, which are based on vector hodographs analysis, for the two-level three-phase voltage inverter fed induction motor drive, are presented. In accordance with the research two diagnostic techniques have been validated experimentally in the direct rotor field oriented control (DRFOC) as well as direct torque control

(DTC) induction motor drive. In contrast to the well known current-based transistor fault diagnostic methods, the conducted study aims to assess the effectiveness, robustness against false alarms and speed of the fault diagnosis of the algorithms based on a rotor or stator flux estimation, depending on the control structure, or method that uses a reference inverter voltage vector. Additionally, simplified implementation schemes of the diagnostic systems have been presented.

Fault diagnostic methods

The analysed IGBT open-circuit faults diagnostic algorithms are dedicated to DRFOC as well as DTC induction motor drive systems with the voltage space vector modulation (SVM). Fig. 1 presents a basic scheme of a two-level voltage source inverter topology, whose faults are considered in accordance with this paper.

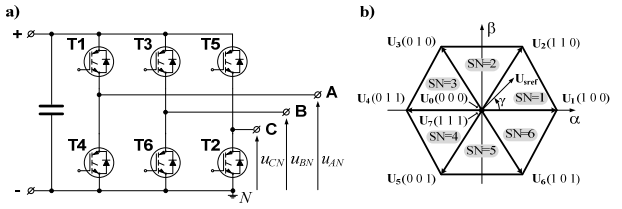

Fig.1. Standard three-phase voltage source inverter: simplified circuit diagram (a), voltage space vectors (b).

To define the transistor fault diagnostic rules, the $\alpha-\beta$ plane is divided into six sectors assigned with the number SN, as following (1):

$$SN_{U,\psi} = \text{int}\left(\frac{\gamma_{U,\psi}}{\pi/3}\right)+1 \tag{1}$$

where *int* means an operation that returns an integer value but γ is an angle, which defined a position of the reference voltage vector $U_{s\,ref}$ in the $\alpha-\beta$ coordinate system.

In case of the first method (M1), a voltage vector presence time t_M is measured in the specific sectors of the complex $\alpha-\beta$ plane [2]. Depending on a direction of the motor rotation and a location of the faulted transistor, in a drive steady state, the reference voltage vector is forced in the one characteristic sector during a much longer time-period than in the case of some other ones. To explain an idea of the method in detail, a block diagram of the transistor fault diagnostic system is shown in Fig. 2.

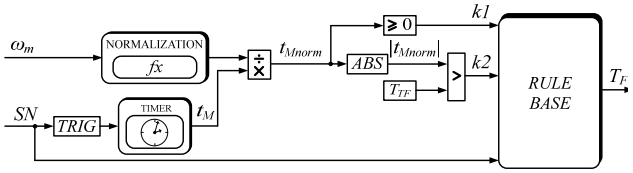

Fig.2. Block diagram of the transitor faults diagnostic system for the method M1

The timer of the system is activated by a triggering event, namely a change of the sector SN_U. Further, a value of an output signal t_M is proportional to a duration when the reference voltage vector is located in the each sectors. As shown in Fig.2, t_M is divided by the output signal of the function defined as (2), which is aimed at a normalization of the diagnostic variable [2].

$$t_{Mnorm} = \frac{t_M}{a\omega_m^{-b}} \tag{2}$$

where t_{Mnorm} means normalized diagnostic signal, ω_m is an angular speed of the motor, T_{timer} is a period of the timer, a=1/T_{timer}, b=1.

The normalization aims to obtain an absolute value of $t_{M\,norm}$ approximately equal to 1 during the drive healthy operation and under its steady states. The failure is detected when the signal $|t_{Mnorm}|$ obtains a fault threshold T_{TF}=1.15. Then, to localize a faulty switch, the rule base, which considers a direction of the motor speed, is utilized, in accordance with the Table 1. Logical variables *k1* and *k2* are the output signals of the comparators of the diagnostic system (see Fig. 2).

Table 1. Open-switch fault symptoms patterns for the first diagnosis technique M1

k1	*k2*	*SN*	***Faulted transistor***
1	1	1	T1
0	1	6	
1	1	2	T2
0	1	1	
1	1	3	T3
0	1	2	
1	1	4	T4
0	1	3	
1	1	5	T5
0	1	4	
1	1	6	T6
0	1	5	

Depending on the control structure, the second considered open-circuit fault diagnostic method (M2) relies on the analyzing of the rotor [29] or stator flux vector amplitude and its position in the $\alpha-\beta$ stationary system. During the healthy mode of the inverter, the absolute value of the estimated rotor flux (in case of DRFOC drive) or the absolute value of the estimated stator flux (for DTC) is approximately constant and equal to the reference value. However, during the power converter faulty mode, once a period of the flux rotational movement, the estimated flux vector absolute value ψ decreases below the nominal value ψ_{ref}, because of asymmetric power supply. An information about the flux vector position, which is defined by an angle γ_ψ, when the control error of ψ is the biggest one and its value is smaller than the fault threshold ψ_{thr} (a local minimum of the time-domain waveform of ψ is observed and its value is smaller than ψ_{thr}) allows to recognize the faulty transistor [29]. The rule base, which considers a direction of the motor speed, is presented in the Table 2. To explain an idea of the method in detail, a block diagram of the transistor fault diagnostic system is shown in Fig. 3.

Table 2. Open-switch fault symptoms patterns for the second diagnosis technique M2

Angular motor speed direction	***Sector SN in which the local minimum of ψ is observed***	**Faulty switch**
positive	1	T1
negative	6	
positive	2	T2
negative	1	
positive	3	T3
negative	2	
positive	4	T4
negative	3	
positive	5	T5
negative	4	
positive	6	T6
negative	5	

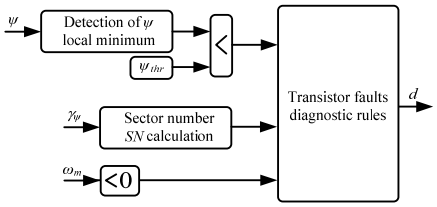

Fig.3. Block diagram of the transistor faults diagnostic system for the method M2

For the rotor flux ψ_r or stator flux ψ_s estimation (3, 4), well known equations based on the mathematic model of the induction machine have been used, respectively [31]:

(3) $$\boldsymbol{\psi}_{\mathbf{s}} = \left(l_s - \frac{l_h^2}{l_r} \right) \mathbf{i}_{\mathbf{s}} + \frac{l_h \boldsymbol{\psi}_{\mathbf{r}}}{l_r}$$

(4) $$\frac{d\boldsymbol{\psi}_{\mathbf{r}}}{dt} = \left(jp_p\omega_m - \frac{r_r}{l_r} \right) \boldsymbol{\psi}_{\mathbf{r}} + \frac{r_r l_h}{l_r} \mathbf{i}_{\mathbf{s}}$$

where: $\mathbf{i_s}$, $\boldsymbol{\psi_s}$ - a vector of stator current and stator flux; $\mathbf{i_r}$, $\boldsymbol{\psi_r}$ - a vector of rotor current and flux; r_s, r_r - a stator and rotor resistance; l_s, l_r, l_h - a stator, rotor and main inductance; ω_k, ω_m - an angular velocity of a coordinate system and an angular rotor speed; p_p - number of pole pairs.

Chosen experimental results

In the following section, chosen experimental results, that validate an effectiveness of the diagnosis methods for IGBT open-circuit failures, are compared. For the study, a laboratory set-up, which a schematic diagram and a picture are presented in Fig. 4a and Fig. 4b, are used. The set-up is built of a 2.2 kW induction machine connected by a stiff shaft to the load machine, namely DC motor with controlled armature current (see Fig. 4b). Nominal parameters of an induction motor are shown in an Appendix 1, in Table 3. A speed of the drive was measured by an incremental encoder (36000 imp./rev.). For the phase currents and DC-link voltage measurement, the LA 55-P and LV 25-P transducers were used, respectively. The control of the drive was carried out with a dSPACE DS1103 rapid prototyping system with the sampling period T_s=100 μs, while the inverter operates at a switching frequency of 4 kHz. For the transistor faults emulation, depending on a required failure location, an appropriate transistor gate command signal was removed.

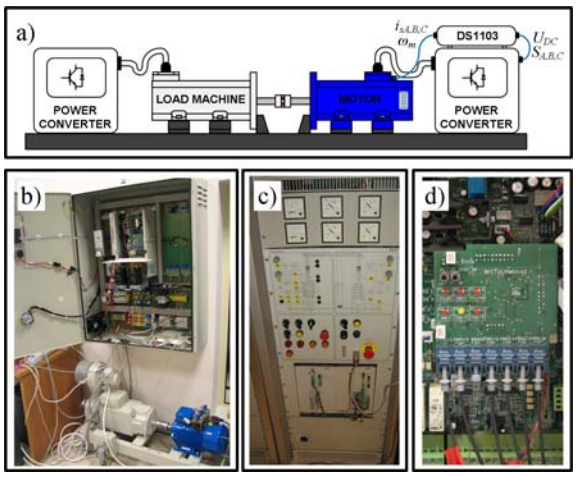

Fig.4. Experimental set-up: a schematic diagram (a), a photo of the induction motor drive (b) the power converter that supplies the DC motor (c) the fiber-optic modules of the inverter (d).

The experimental research, which chosen results are presented in this section, are organized as following. First, the robustness of the algorithms against false alarms under harsh transients of a drive speed and rapid changes of the load torque was validated. Moreover, during these tests the fault thresholds required for the correct fault diagnosis have been obtained. After that, the IGBT open-circuit faults are emulated during a constant reference motor speed n_{ref}. Next, the methods are tested for the faults occurring during motor speed linear changes. Finally, the speed of the diagnosis was compared for the each methods taking into consideration a failure instant related to the phase of the current. In all figures, a pink dotted line marks an instant of the single switch open-circuit fault occurrence but a moment of the failure localization is marked as a blue dotted line. In order to rate a time, that is required to conduct the transistor fault diagnosis, a normalized fault localization time t_D is defined as a part of a stator current period T_i that is measured before the fault applying. Additionally, in figures is presented the speed of the drive n, phase currents $i_{sA,B,C}$ and chosen diagnostic variables, depending on the tested method. In case of M1, time-domain waveforms of the signal $|t_{Mnorm}|$ and the SN_U, which means the sector, that defined the position of the reference voltage vector in the stationary system, are shown. Moreover, transients of the rotor ψ_r or stator ψ_s flux absolute value and the flux vector position described by the sector number SN_ψ are presented.

Fig. 5 and Fig. 6 show the transients of the measured motor speed n, stator currents $i_{sA,B,C}$ and diagnostic variables $|t_{Mnorm}|$ and ψ_s or ψ_r, depending on the tested control structure (Fig. 5 corresponds to the DTC-SVM and Fig. 6 to the DRFOC-SVM), during harsh transient of the motor speed and rapid changes of the load torque (from no-load to the full load). These tests have allowed to assume the transistor fault indicating thresholds: T_{TF}=1.15 for the M1, with no regard to the control structure, $\psi_{s\,thr}$=0.88 and $\psi_{r\,thr}$=0.95, so that the values of the diagnostic variables do not exceed these thresholds during the drive healthy operation mode.

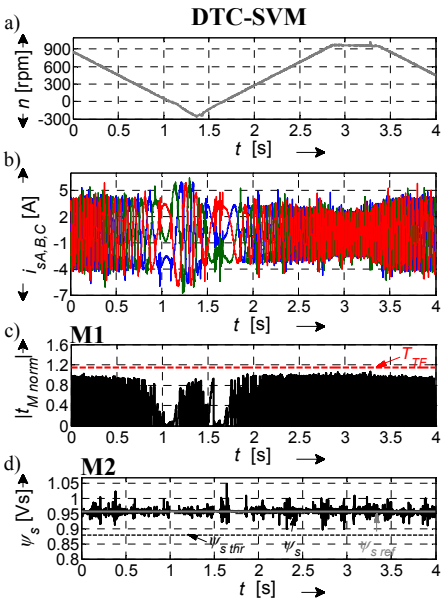

Fig.5. Experimental results regarding the fault threshold fitting process with the time-domain waveforms of the speed (a), stator currents (b), diagnostic variables related to the 1st method $|t_{Mnorm}|$ (c) and the absolute value of the stator flux ψ_s the machine (d) for the DTC-SVM.

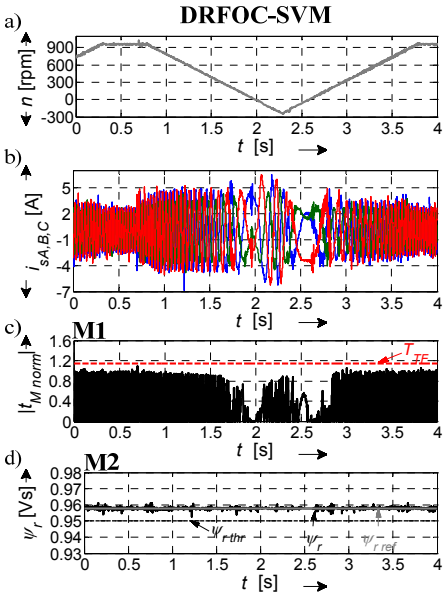

Fig.6. Experimental results regarding the fault threshold fitting process with the time-domain waveforms of the speed (a), stator currents (b), diagnostic variables related to the 1st method $|t_{Mnorm}|$ (c) and the absolute value of the rotor flux ψ_r of the machine (d) for the DRFOC-SVM.

Fig.7 and Fig.8 present experimental results achieved for the T1 failures that were occurred for the same current phase angle γ_i=π/3, when the drive operated with the constant reference speed n_{ref}=720 rpm and the load torque m_L=7.2 Nm. In case of DTC, the fault was applied at the instant t=0.028 s.

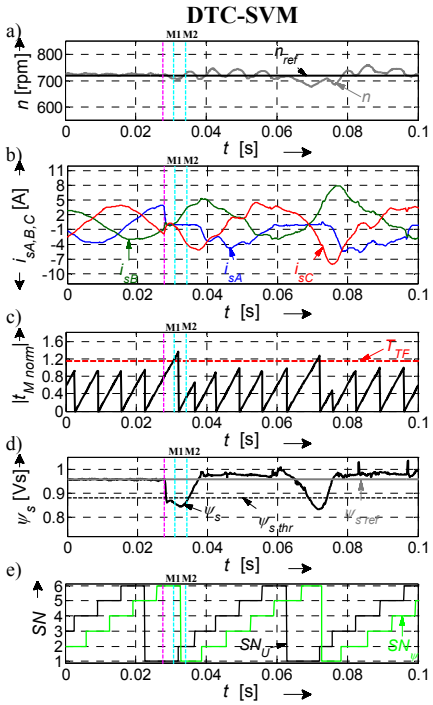

Fig.7. Experimental results concerning the transients of the drive speed (a), stator currents (b), the diagnostic variables (c, d, e) for a single power switch open-circuit fault in T1, in case of DTC-SVM.

As can be seen in Fig.7c, at t=0.031s the diagnostic signal $|t_{Mnorm}|$ exceeded the fault threshold T_{TF}=1.15, when the inverter voltage vector was located in the 1st sector of the α–β plane (see Fig. 7e SN_U=1), so the fault localization time comprises 0.08 of the current fundamental period (t_D=0.08T_i). In case of the second transistor fault diagnostic method (M2), the local minimum of the ψ_s was detected at t=0.035 s (see Fig. 7d), when the stator flux vector was located in the 1st sector of the α–β plane (see Fig. 7e SN_ψ=1). The fault localization time comprises 0.19 of the current fundamental period (t_D=0.19T_i) and it is longer than for the method M1. Compared to the previously considered case, Fig. 8 shows results related to the DRFOC. At t=0.016 s the T1 open-circuit fault was applied and the faulted transistor was recognized at t=0.019 s, in case of M1 but for the method M2, the failure was localized at t=0.025 s. In both considered cases, the fault localization time t_D is less than one current fundamental period, namely t_D =0.08 T_i for M1 and t_D =0.03 T_i for M2.

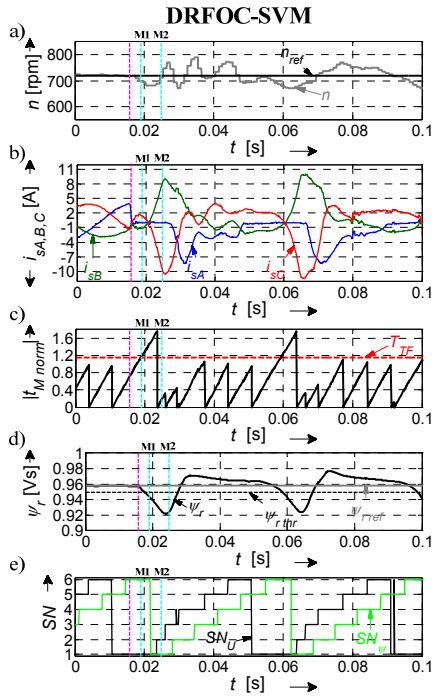

Fig.8. Experimental results concerning the transients of the drive speed (a), stator currents (b), the diagnostic variables (c, d, e) for a single power switch open-circuit fault in T1, in case of DRFOC-SVM.

Fig. 9 and 10 show the experimental results, which correspond to the transistor faults that occurred during linear changes of the drive speed n_{ref}=720 rpm and the load torque m_L=7.2 Nm. First, at the time t =0.02 s the open-circuit fault in the T1 transistor was introduced during the motor speed-deceleration in DTC structure. Unlike the previous case, the results are related to DRFOC. The fault of T4 was applied at t =0.31 s. As with the both tests, the fault diagnostic time t_D is shorter than the one current fundamental period, namely t_D =0.44 T_i for M1 and t_D =0.32 T_i in case of T1 failure (see Fig. 9) and t_D =0.21 T_i for M1 t_D =0.13 T_i in case of the T4 failure (see Fig. 10).

In Fig. 11 summarized test results, which correspond to the speed of the T1 open-circuit fault diagnosis depending on the failure instant, that has been defined by the phase angle □$_i$ of the current i_{sA}. This research has representative character and was conducted under constant reference speed, which value was equal to the half of the nominal motor speed n_{ref}=0.5n_N and for the medium load torque m_L=0.5m_N.

The obtained results have proved that in case of both analyzed methods the time, that is required to the transistor fault diagnosis, is shorter than one period of the stator current fundamental harmonic, with no regard to the failure instant. Taking into account the methods known from

literature, which have been briefly discussed in the paper introduction, for example [17], the proposed diagnostic techniques are competitive. Additionally, it is visible that in case of the first algorithm (M1), the transistor fault diagnosis takes less time than it is required to find the faulted transistor by utilizing the second approach (M2).

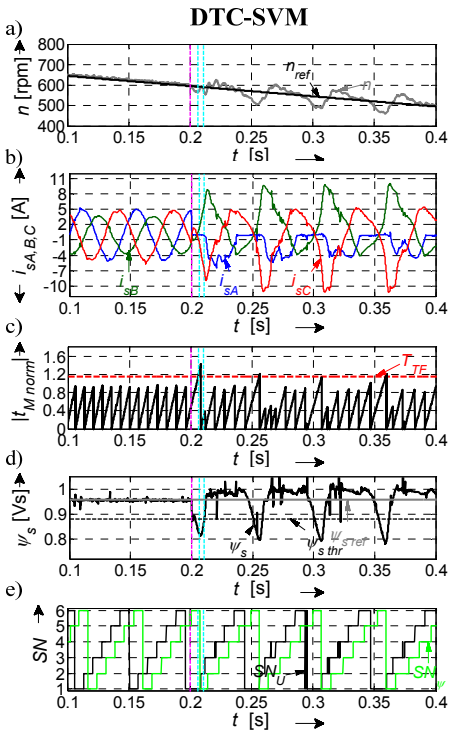

Fig.9. Experimental results concerning the transients of the drive speed (a), stator currents (b), the diagnostic variables (c, d, e) for a single power switch open-circuit fault in T1, that occured during lineral speed changes, in case of DTC-SVM.

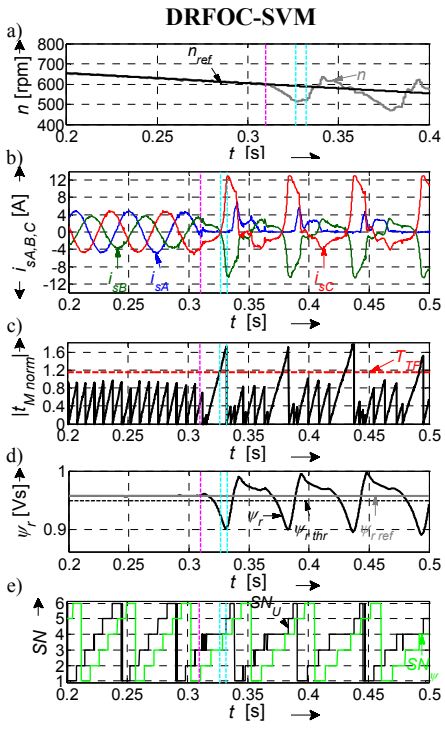

Fig.10. Experimental results concerning the transients of the drive speed (a), stator currents (b), the diagnostic variables (c, d, e) for a single power switch open-circuit fault in T4, that occured during lineral speed changes, in case of DRFOC-SVM.

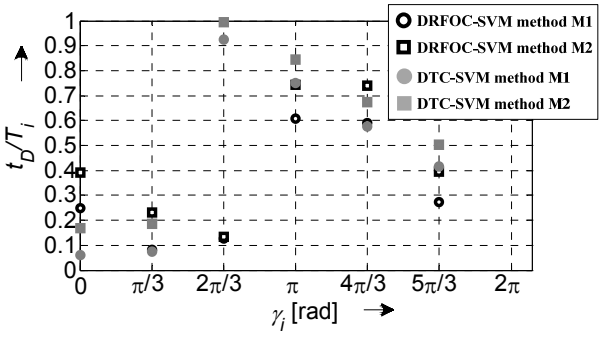

Fig.11. Speed of the open-circuit fault diangosis depending on the current phase angle γ_i of the faulty inverter phase, for the analyzed method M1 and M2, in case of the DTC-SVM or DRFOC-SVM.

Conclusions

This paper has treated the comparison of the low-cost diagnostic methods for the single power switch open-circuit faults of the two-level three-phase voltage inverters, which operate in DTC-SVM as well as DRFOC-SVM motor drive system. The idea of the fault diagnostic techniques consist in analyzing of vector hodographs of easy assessable signals, without using additional hardware. The main achievement of this work is selection of accurate diagnostic signals, which are used for the transistor failures localization and a design of effective diagnostic algorithms, which require low computational power and tune effort.

The proposed diagnostic methods ensure the correct single-switch open-circuit fault diagnosis in a time shorter than one period of the stator current fundamental harmonic without regard to a drive operation point.

The main advantage of the method is the full robustness against false alarms and a simple hardware implementation, which can be realized by using microprocessor systems.

Appendix 1

Table 3. Data of induction motor

Rated data		
Quantity	***Symbol***	***Value***
Power	P_N	2.2 kW
Torque	m_N	14.6 Nm
Speed	n_N	1440 rpm
Voltage	u_N	400 V
Current	i_N	4.5A

This research work was supported by National Science Centre (Poland) under project DEC-2013/09/B/ST7/04199

***Author**: Piotr Sobański, M.Sc., Wrocław University of Technology, Department of Electrical Machines, Drives and Measurements, ul. Wybrzeże Wyspiańskiego 27, 57-370 Wrocław, piotr.sobanski@pwr.wroc.pl*

LITERATURA

[1] Yang S., Xiang D., Bryant P., Ran L., Tavner P., Condition monitoring for device reliability in power electronic converters: a review, *IEEE Trans. on Power Electronics*, 25 (2010), 2734-2752

[2] Orlowska-Kowalska T., Sobanski P., Simple Sensorless Diagnosis Method for Open-Switch Faults in SVM-VSI-fed Induction Motor Drive, *IEEE 39th Ann. Conf. of the Ind. Electron. Soc.*, (2013), 8210–8215

[3] Alavi M., Wang D., Luo M., Short-Circuit Fault Diagnosis for Three-Phase Inverters Based on Voltage-Space Patterns, *IEEE Trans. on Ind. Electron.*, 61 (2014), 5558–5569

[4] Kwang-Woon L., Myungchul K., Jangho Y, Kwang-Woon L., Ji-Yoon Y., Condition Monitoring of DC-Link Electrolytic Capacitors in Adjustable-Speed Drives, *IEEE Trans. on Ind. App.*, 44 (2008), 1606–1613

[5] Smet V., Forest F., Huselstein J.-J., Richardeau F., Khatir Z., Lefebvre S., Berkani M., Ageing and Failure Modes of IGBT

Modules in High-Temperature Power Cycling, *IEEE Trans. on Ind. Electron.*, 58 (2011), 4931–4941
[6] Rodríguez-Blanco M.A., Claudio-Sánchez A., Theilliol D., Vela-Valdés L.G., Sibaja-Terán P., Hernández-González L., Aguayo-Alquicira J., A Failure-Detection Strategy for IGBT Based on Gate-Voltage Behavior Applied to a Motor Drive System, *IEEE Trans. on Ind. Electron.*, 58 (2011), 1625–1633
[7] Estima J.O., Cardoso A.J.M., Fast fault detection, isolation and reconfiguration in fault-tolerant permanent magnet synchronous motor drives, Energy Convers. Congr. and Expos., (2012), 3617–3624
[8] Zhang W., Xu D., Enjeti P.N., Li H., Hawke J.T., Krishnamoorthy H.S., Survey on Fault-Tolerant Techniques for Power Electronic Converters, *IEEE Trans. on Pow. Electron.*, 29 (2014), 6319–6331
[9] Choi U., Lee K., Blaabjerg F., Lee K., Reliability Improvement of a T-Type Three-Level Inverter With Fault-Tolerant Control Strategy, *IEEE Trans. on Pow. Electron.*, (2015), 2660–2673
[10] Garg P., Essakiappan S., Krishnamoorthy H.S., Enjeti P.N., A Fault-Tolerant Three-Phase Adjustable Speed Drive Topology With Active Common-Mode Voltage Suppression, *IEEE Trans. Pow. Electron.*, 30 (2015), 2828–2839
[11] Orlowska-Kowalska T., Sobanski P., Survey on two-level voltage inverters robust to IGBT faults (in Polish), *Scientific Papers of the Institute of Electrical Machines, Drives and Measurements of the Wrocław University of Technology. Studies and Research*, 33 (2013), 54-69
[12] Trabelsi M., Boussak M., Mestre P., Gossa M., An improved diagnosis technique for IGBTs open-circuit fault in PWM-VSI-fed induction motor drive, *IEEE Int. Symp. Ind. Electron.*, (2011), 2111-2117
[13] Jung Shin-Myung, Park Jin-Sik, Kim Hyoung-Suk, Kim Hag-Wone, Youn Myung-Joong, Simple switch open fault detection method of voltage source inverter, *IEEE Energy Conv. Congress and Exp.*, (2009), 3175-3181
[14] An Qun-Tao, Sun Li-Zhi, Zhao Ke, Sun Li, Switching Function Model-Based Fast-Diagnostic Method of Open-Switch Faults in Inverters Without Sensors, *IEEE Trans. Pow. Electron.*, 26 (2011), 119-126
[15] Alavi M., Luo M., Wang D., Bai H., IGBT fault detection for three phase motor drives using neural networks, *17th Conf. on Emerging Technol. and Factory Autom.*, (2012), 1-8
[16] Lee C., Choi W., Design and evaluation of voltage measurement based sectoral diagnosis method for inverter open switch faults of permanent magnet synchronous motor drives, *IET–Electric Power Applications*, 6 (2012), 526-532
[17] Estima J.O., Freire N.M.A., Cardoso A.J.M., Recent advances in fault diagnosis by Park's vector approach, *IEEE Workshop on Electr. Mach. Des. Control and Diagn.*, (2013), 279-288
[18] Sleszynski W., Nieznanski J., Cichowski A., Open-Transistor Fault Diagnostics in Voltage-Source Inverters by Analyzing the Load Currents, *IEEE Trans. on Industry Appl.*, 56 (2009), 4681–4688
[19] An Q., Sun L., Sun L., Current Residual Vector-Based Open-Switch Fault Diagnosis of Inverters in PMSM Drive Systems, *IEEE Trans. on Pow. Electron.*, (2015), 2814-2827
[20] Estima J.O., Marques Cardoso A.J., A New Algorithm for Real-Time Multiple Open-Circuit Fault Diagnosis in Voltage-Fed PWM Motor Drives by the Reference Current Errors, *IEEE Trans. on Ind. Electron.*, (2013), 3496-3505
[21] Jlassi I., Estima J.O., El Khil S.K., Bellaaj N.M., Marques Cardoso A.J., "Multiple Open-Circuit Faults Diagnosis in Back-to-Back Converters of PMSG Drives for Wind Turbine Systems", *IEEE Trans. on Pow. Electron.*, 30 (2015), 2689–2702
[22] Freire N.M.A., Estima J.O., Cardoso A.J.M., A voltage-based approach for open-circuit fault diagnosis in voltage-fed SVM motor drives without extra hardware, Int. Conf. on Electr. Mach., (2012), 2378-2383
[23] Peuget R., Courtine S., Rognon J.P., Fault detection and isolation on a PWM inverter by knowledge-based model, *IEEE Trans. Ind. Appl.*, 34 (1998), 1318-1326
[24] Sleszynski W, Nieznanski J., Cichowski A., Real-time fault detection and localization vector-controlled induction motor drives, *11th Europ. Conf. Pow. Electr. and Appl.*, (2005), 2-8
[25] Trabelsi M., Boussak M., Gossa M., Multiple IGBTs open circuit faults diagnosis in voltage source inverter fed induction motor using modified slope method, *19th Int. Conf. Electr. Mach.*, (2010), 1-6
[26] Rivelino Espinoza-Trejo D., Campos-Delgado D.U., Bossio G., Bárcenas E., Hernández-Díez J.E., Lugo-Cordero L.F., Fault diagnosis scheme for open-circuit faults in field-oriented control induction motor drives, *IET Pow. Electron.*, 5 (2013), 869-877
[27] Campos-Delgado D.U., Pecina-Sánchez J.A., Rivelino Espinoza-Trejo D., Román Arce-Santana E., Diagnosis of open-switch faults in variable speed drives by stator current analysis and pattern recognition, *IET Electric Pow. Appl.*, 8 (2013), 509-522
[28] Orlowska-Kowalska T., Sobanski P., Simple diagnostic technique of a single IGBT open-circuit faults for a SVM-VSI vector controlled induction motor drive, *Bull. of the Pol. Acad. of Sci. Tech. Sci.*, 63 (2015), 281–288
[29] Sobanski P., Fuzzy-logic-based approach to voltage inverter fault diagnosis in induction motor drive, *Przegląd Elektrotechniczny*, 90 (2014), 149-153
[30] Sobanski P., Orlowska-Kowalska T., Simple transistors fault localization algorithm for voltage inverter-fed induction motor drive (in Polish), *Scientific Papers of the Institute of Electrical Machines, Drives and Measurements of the Wrocław University of Technology. Studies and Research*, 34 (2014), 76-85
[31] Holtz J., The dynamic representation of AC drive systems by complex signal flow graphs, *IEEE Int. Symp. on Ind. Electron.*, (1994),1-6